Microchimica Acta (2018) 185: 137
https://doi.org/10.1007/s00604-018-2685-x

ORIGINAL PAPER

Determination of norfloxacin or ciprofloxacin by carbon dots fluorescence enhancement using magnetic nanoparticles as adsorbent

Jianhao Hua[1] · Yang Jiao[2] · Meng Wang[1] · Yaling Yang[1]

Received: 14 November 2017 / Accepted: 15 January 2018 / Published online: 27 January 2018

Abstract

The authors describe a method for the determination of norfloxacin (NOR) or ciprofloxacin (CIP). It is making use of a combination of fluorescence enhancement and magnetic solid-phase extraction (MSPE). Sulfur-doped carbon dots (S-CDs) are used as a fluorescent probe. They were prepared by a one-pot method using poly(4-styrenesulfonic acid-co-maleic acid) (PSMA) as a source for carbon and sulfur. NOR or CIP act as sensitizers of fluorescence (with excitation/emission maxima at 324/412 nm), probably due to strong hydrogen bond interaction and charge transfer with the S-CDs. The S-CDs were characterized by using TEM, XRD, XPS, FT-IR, UV-Vis and fluorescence spectroscopies. Response is linear in the 0.02–1.25 μM NOR concentration range, and the detection limit is 4.6 nM. The respective data for CIP are 0.02–1.0 μM and 6.7 nM. The average recoveries of NOR and CIP residues from spiked bovine raw milk are 96.2%~105.2% and 92.3%~102.5%.

Keywords Fluoroquinolones · Nanomaterials · Fluorescent probe · Surface states · Sulfonic acid · Bovine raw milk · Magnetic solid-phase extraction

Introduction

Fluoroquinolones (FQs) are widely applied as veterinary and human medicines to fight against many Gram negative and Gram positive organisms [1]. Among fluoroquinolones, norfloxacin (NOR) and ciprofloxacin (CIP) are the most widely used antibiotics [2]. Antibiotics residues have been found in a wide range of environmental surface water and food. Especially, their residues in milk products have reported and drew wide attention. Long-term exposure to such milk products contaminated with FQs residues can lead to an increased allergic reactions, liver damage, gastrointestinal disturbance and drug-resistance of microbial strains [3–6]. Consequently, monitoring of FQs residues is a crucial issue.

To date, a variety of methods have been applied for determining FQs residues, which include liquid chromatography/post-column derivatization [7], surface enhanced Raman spectroscopy (SERS) detection [8], liquid chromatography with fluorescent detection (LC-FLD) [9], liquid chromatography-electrospray ionization-tandem mass spectrometry (LC-ESI-MS/MS) [10], voltammetric [11], chemiluminescence [12], colorimetry [1], spectrofluorimetric detection [13–15]. The widely used HPLC methods or LC-ESI-MS/MS for the determination of NOR and CIP or similar fluoroquinolone in complex matrices involve tedious clean-up steps prior to chromatography, as well requirement of sophisticated instrumentation and time consumption. Also, ordinary spectrometric detection can't be applied to complex food-based matrices.

Carbon dots (CDs) are considered as one of the most extensively optical nanomaterials in the last few years [16, 17]. They exhibit excellent properties including outstanding water solubility, good biocompatibility, low toxicity, robust chemical inertness and ease of preparation [18–21]. These advantages make CDs superior to classic fluorescent molecules and the reported fluorescent nanoprobes based on CDs focused on the bioimaging [22], detection of metal ions [23], protein [24], hormone [25], glucose [26] and other small molecules [27, 28]. Theoretically, any phenomenon of fluorescence change (intensity, wavelength, anisotropy, or lifetime) related to the

Electronic supplementary material The online version of this article (https://doi.org/10.1007/s00604-018-2685-x) contains supplementary material, which is available to authorized users.

✉ Yaling Yang
yilyil8@163.com

[1] Faculty of Life Science and Technology, Kunming University of Science and Technology, Kunming, Yunnan Province 650500, China

[2] Department of Civil and environmental engineering, Carnegie Mellon University, Pittsburgh, PA 15213, USA

concentration of different analytes demonstrates the potential to be used as probes. The mechanism of assay is significant for fluorescent probes, the conventional mechanisms include fluorescence resonance energy transfer (FRET), twisted intramolecular charge transfer (TICT), electronic energy transfer (EET), intramolecular charge transfer (ICT), and photo-induced electron transfer (PET), photo-induced charge transfer (PCT), inner filter effect (IFE) [29–32].

In general, spectrofluorimetric detection, because of its simplicity and rapidity, the method has already been described for determination of FQs through sensitization of fluorescence. According to the previous literature [33], in order to accurately recognize target molecule in complex matrix at trace levels, magnetic solid-phase extraction (MSPE) was used as a preconcentration method. In addition, CDs are hydrophilic, which provides a good opportunity to produce hydrogen bonds with analytes [34, 35]. Strong hydrogen bonds only include F- H…F^-, O –H…O^- and O^+ -H…O, which are always a few two-center bonds of short distances and are directional, with energies higher than 41 kJ·mol^{-1} [36]. Herein, we present a novel strategy to detect NOR or CIP residues by carbon dots fluorescence enhancement. Fluorescent intensity of the S-CDs is enhanced by norfloxacin or ciprofloxacin based on strong hydrogen bond interaction and charge transfer, it's the theoretical basis in our work. It should be pointed out that this is the first time that there has been report on the use of fluorescent S-CDs for detection of NOR or CIP residues in real sample matrices coupled with magnetic solid-phase extraction. This method exhibits many advantages, for instance, environmentally friendly, improvements in automation, short time requirement, reduced solvent consumption.

Experimental section

Reagents and materials

Poly(4-styrenesulfonic acid-co-maleic acid) (PSMA), norfloxacin (NOR), ciprofloxacin (CIP), ofloxacin (OFL), difloxacin (DIF), fleroxacin (FLE), pefloxacin (PEF), enoxacin (ENO) and levofloxacin (LEV) were purchased from Aladdin Chemistry Co. Ltd. (http://www.aladdin-e.com/). Citric acid (CA), dibasic sodium phosphate (Na_2HPO_4), sodium hydroxide (NaOH), hydrochloric acid (HCl), sodium dodecyl sulfate (SDS), 2-(5-bromo-2-pyridylazo)-5-(diethylamino)phenol (5-Br-PADAP) were purchased from Sinopharm Chemical Reagent Co., Ltd. (http://www.sinoreagent.com/). Ferric chloride ($FeCl_3$•$6H_2O$), ammonium ferrous sulfate ($(NH_4)_2Fe(SO_4)_2$•$6H_2O$), ammonia solution (NH_3•H_2O), methanol and ethanol were supplied by Tianjin Fengchuan Chemical Reagent Co., Ltd.(http://www.tjhxsj.cn/). Standard stock solutions of NOR and CIP were prepared by double distilled water containing 10 mM HCl. They were all stored at 4 °C in the dark and can be stable for 2 months, the working solutions were obtained by appropriate dilution of the stock solutions with double distilled water. All Chemicals used were at least of analytical reagent grade and were used without further purification.

Apparatus

The UV-Vis absorption spectrum of CDs was recorded by a UV-2600 UV-Vis spectrophotometer (SHIMADZU, Japan). Fluorescence measurements were carried out on a G9800A Cary Eclipse fluorescence spectrophotometer (Agilent Technologies, USA). The images of particle CDs were obtained by a Tecnai G2 F30 transmission electron microscope (TEM) (FEI, USA) at 200 kV. The functional groups on the CDs were measured with a TENSOR27 Fourier transform infrared spectroscopy (FT-IR) spectrometer (Bruker, Germany). Other instruments including: a D8-advance X-ray diffractometer (XRD) (Bruker, Germany), a Thermo Scientific K-Alpha X-photoelectron spectroscopy (XPS) (Thermo Fisher Scientific Inc. U.S.A.), a vortex mixer (Hanuo Instrument Co., Ltd., XH-B, Shanghai, China), high speed centrifuge (Shanghai Surgical Instrument Factory, 80–2, Shanghai, China), vacuum drying oven BPZ-6033 (Shanghai, China), a digital display temperature control water-bath Model XMTB (Central Experimental Furnace Co., Ltd., Tianjin, China), a pH meter pHS-3C (Shanghai Leici Instruments Factory, China) .

Preparation of S-CDs

The hydrothermal synthesis of S-CDs is described as follows: Poly(4-styrenesulfonic acid-co-maleic acid) (3.0 g) was dissolved in deionized water (100 mL). The solution was transferred into a teflon-lined stainless steel autoclave (150 mL) and heated at 220 °C for 5 h. After the reaction, the autoclave was taken out from the oven and cooled to room temperature naturally. The yellow aqueous solution was purified by filtration through 0.22 μm filter and then centrifuged at 10,000 rpm for 15 min to remove large particles, stored at 4 °C before used (quantum yield measurement details is displayed in Electronic Supplementary Material).

Preparation of milk samples

Bovine raw milk was purchased from a local farm in Kunming City (Yunnan Province, China). Preliminary analyses showed that no FQs residues were present to disturb the preparation of matrix-matched calibration standards and spiked samples for the validation of the method. For the precipitation of proteins and extraction of residual drugs, 50 mL of bovine raw milk sample was heated to 40 °C in a water bath. 0.5 M HCl was added slowly into the sample described above under continuously stirring, the pH of the sample solution should be adjusted to 4.7. The

resulting suspension cooled to room temperature naturally, then centrifuged at 4000 rpm for 5 min to remove precipitation of proteins. Sample solution was stored at 4 °C before used.

MSPE procedure

In a typical process, magnetic nanoparticles (MNPs) were synthesized by the in situ chemical coprecipitation (see details in Electronic Supplementary Material). The MSPE procedure was carried out as follows: 120 μL of the above MNP suspension was added to 5 mL sample solution. The mixture was vortex-mixed for 120 s to make NOR or CIP fully adsorbed by the MNPs. Then, MNPs were separated quickly from the sample solution by using an external magnet, the supernatant was decanted and the MNPs were eluted by 50 μL of methanol. Finally, the eluate was isolated from MNPs by using an external magnet and combined with S-CDs for subsequent spectrofluorimetric detection analysis.

Detection of NOR and CIP

As shown in Fig. 1a, determination of NOR and CIP was performed in phosphate buffer (PB) (30 mM, pH 6.0) at room temperature. The standard stock solution of NOR and CIP was prepared by dissolving the appropriate amount of norfloxacin (NOR) and ciprofloxacin (CIP). In a typical run, 25 μL S-CD solution, 500 μL of PB and different amounts of NOR or CIP were added into a 10.0 mL colorimetric tube, and the mixture was diluted to 4.0 mL with ultrapure water and vortex-mixed for 1 min to mix completely before spectral measurements. The fluorescence spectra were collected with excitation/emission maxima at 324/412 nm, and the slit widths

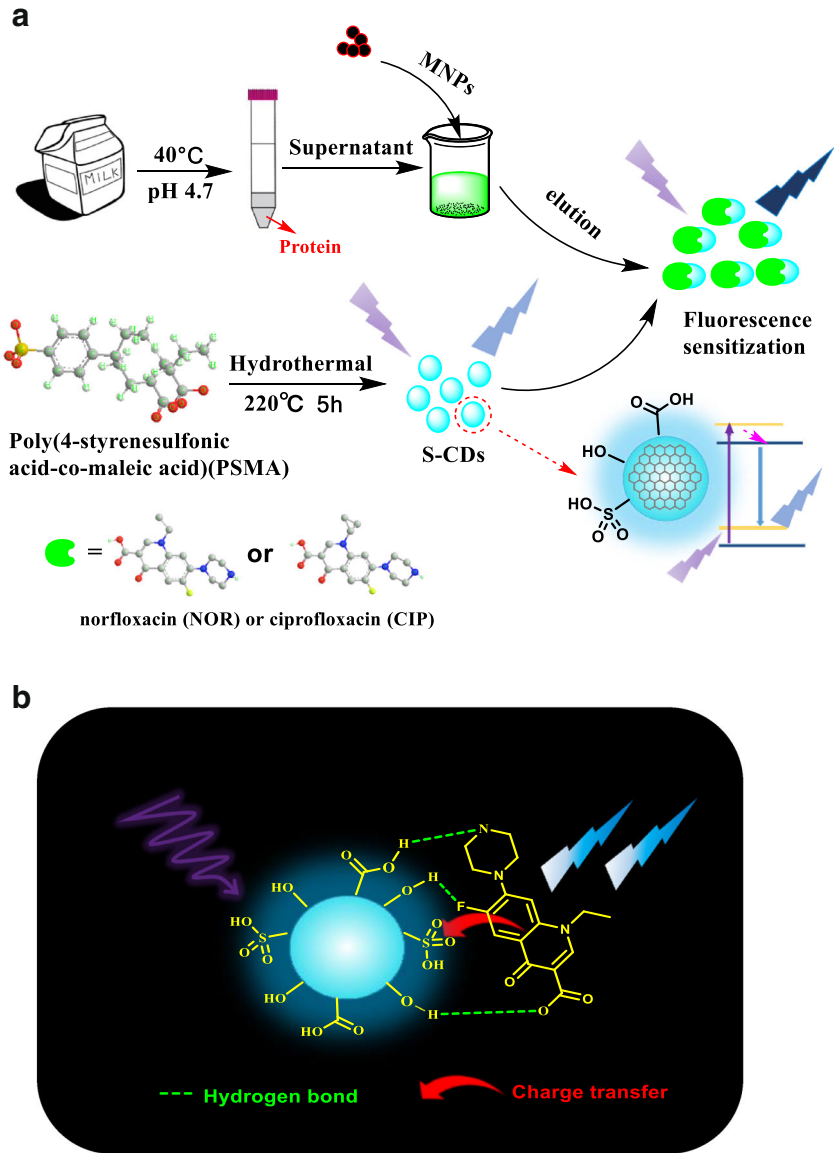

Fig. 1 a Processing diagram for the norfloxacin and ciprofloxacin determination process. b Schematic illustration of carbon dots fluorescence enhancement

of the excitation and emission were both 5 nm. In order to assess the influence of co-existing interferences on the fluorescence of S-CDs and evaluate the selectivity for NOR or CIP, the similar procedure was performed for the detection of other fluoroquinolones: ofloxacin (OFL), difloxacin (DIF), fleroxacin (FLE), pefloxacin (PEF), enoxacin (ENO), levofloxacin (LEV).

Results and discussion

Choice of materials

Carbon dots (CDs) are promising in fluorescent assays, but they are limited in various areas of applications [37]. Particularly, heteroatom-doping results in a significant improvement in electronic and fluorescence properties of CDs. Several strategies have been reported in the literature on the doping of CDs with various heteroatoms such as N, S, B or P [25, 38]. According to the previous literature [39], in order to broaden their applications in analysis and probes, S-CDs were synthesized from S-containing polymer precursors. The fluorescence capability of the S-CDs was related to the specific configuration of the heteroatoms. S-CDs do not differ significantly in the surface chemistry from other CDs, and sulfonic acids acting as chromophores played the most important role. Sulfonyl plays a pivotal role in S-CDs acting as sensitive and selective assay towards NOR and CIP. Consequently, poly(4-styrenesulfonic acid-co-maleic acid) was selected to be polymer precursors.

Characterization of S-CDs

The transmission electron microscopy (TEM) technique was used to explore the morphology and particle size distributions of S-CDs. As shown in Fig. 2a and Fig. S1, the S-CDs had high dispersity and uniform spherical shapes, and with a size distribution within the range of 3–10 nm and an average diameter of about 5.4 nm.

The surface chemistry of S-CDs was studied using Fourier transform infrared (FT-IR) spectroscopy. The typical FT-IR spectra of S-CDs was shown in Fig. 2b. As can be seen, a broad peak at 3456 cm^{-1} reveals the existence of O–H stretching vibrations of hydrogen bond. Several sharp peaks at 1180 cm^{-1}, 1122 cm^{-1}, 1042 cm^{-1} correspond to –C(=S)– stretching vibrations, respectively. Characteristic absorption bands can be observed for the $–COCH_2–$ bending vibration mode at about 1405 cm^{-1}. Also, the peak appearing at 1581 cm^{-1} may be caused by the asymmetric and symmetric stretching vibration of COO^-. They can be assigned to the existence of carboxyl bending. In addition, the absorptions at 2939 and 618 cm^{-1} display C–H stretching vibrations, these results indicate the generation of S-CDs.

The XPS spectrum provided more convincing evidence for elemental contents and surface groups of S-CDs. As shown in Fig. S2a, the full scan XPS spectra presented distinct peaks locating at 197.6, 220.0, 283.2 and 533.6 eV, which are attributed to S2P, S2S, C1s and O1s, respectively. This further corroborated that the S-CDs mainly contained carbon, sulfur, and oxygen. The high resolution spectrum of C1s (Fig. S2b) displayed four different types of surface components, corresponding to C–C/C=C at binding energies of 283.0 eV, C–S at 283.8 eV, and O–C=O at 287.0 eV. In addition, the high resolution spectrum of S2P (Fig. S2c) was fitted with two peaks at 167.2 eV and 168.3 eV, which are ascribed to S=O and S–C bonds. The high resolution O1s spectrum of S-CDs (Fig. S2d) is fitted with three peaks at 530.4 eV, 531.2 eV and 534.8 eV, which are ascribed to C–O, C=O and S=O bonds. The surface components of S-CDs determined by the XPS were in agreement with that of FT-IR results. According to the FT-IR and XPS results, sulfur was co-doped in CDs, and their related functional groups, including carboxyl, hydroxyl and sulfonyl existed on their surface (X-ray diffraction (XRD) pattern details is displayed in Electronic Supplementary Material).

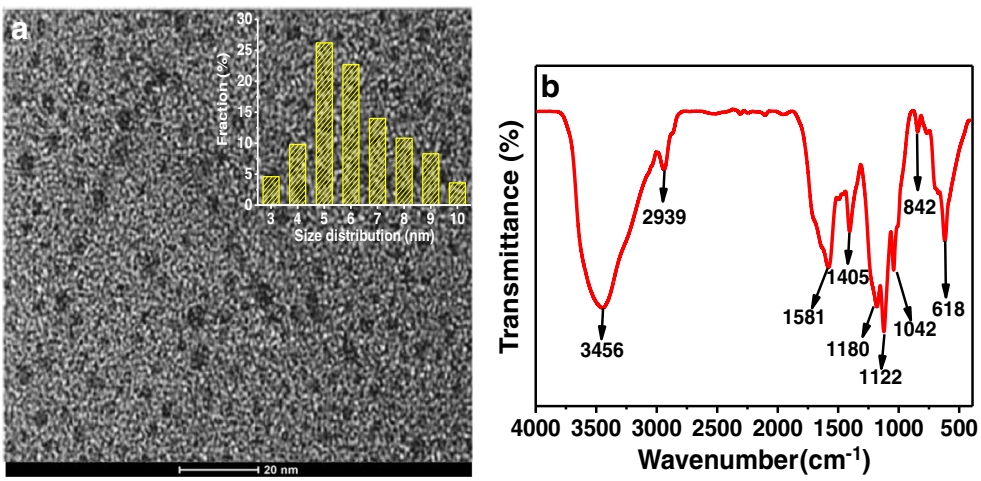

Fig. 2 a The TEM image of the S-CDs drop casted on copper grid (inset: size distributions). b FT-IR spectra of S-CDs

Spectroscopic properties of S-CDs

To explore the optical properties of the S-CDs, UV-Vis absorption spectra and fluorescence spectra of the S-CDs in aqueous solution were investigated as shown in Fig. 3. It was observed that a characteristic UV-Vis strong absorption peak was located at 262 nm (Fig. 3a). The optical absorption peak was typically assigned to the n–π* transition and the contribution of surface moieties. The electron-rich nature of unsaturated groups with sulfur atoms changed the charge density of S-CDs, resulting in the energy transfer to the excited π* state of the sp^2 cluster of S-CDs. As shown in Fig. 3b, the maximum emission intensity is centered at 412 nm with an excitation wavelength of 324 nm (QY = 12%). The S-CD solution is faint yellow under daylight and emit a brighter blue fluorescence under the excitation of 365 nm UV light. Moreover, the S-CDs exhibited excitation-dependent fluorescence behavior. As shown in Fig. S4, when the excitation wavelength increased from 264 nm to 404 nm, the fluorescence emission peak was obviously shifted to longer wavelength with variable fluorescence intensity. It may be attributed to different sized carbon nanoparticles in the S-CD solution, these excitation tunable emission spectra are considered to be the versatile characteristic of S-CDs. This property may be due to quantum confinement, size distribution or the presence of emissive traps on the surface.

Optimization for the magnetic solid-phase extraction conditions

Several parameters, including the amount of MNPs, the vortex extraction time for adsorption, sample solution pH, and desorption conditions were investigated to achieve the best extraction efficiency. All the experiments were performed in triplicate and the means of the results were used for optimization. In summary, based on the all optimization results, the addition of 120 μL MNP suspension, vortex for 2 min for NOR and 1.5 min for CIP, pH 6.0, elution with only 50 μL methanol for NOR and CIP were employed for the following studies.

Analysis of fluorescence enhancement mechanisms

The fluorescence enhancement mechanisms may attribute to the valuable phenomenon of hydrogen bond interaction and charge transfer between S-CDs and NOR or CIP. On the one hand, taking into account the structural similarity of NOR and CIP, as well their structure-reactivity relationship toward S-CDs. As shown in Fig. 1b, the fluorescent probe can be associated with surface states. In accordance with characterization of S-CDs, the unique assay properties of S-CDs arise from the combination of material and dimensionality. The large surface area-to-volume ratios of S-CDs, and it contains abundant carboxyl, hydroxyl and sulfonyl groups. These advantages provide aqueous solubility and opportunities for combination with NOR or CIP based on hydrogen bond interaction. The special and strong hydrogen bond may occur between the carboxyl of S-CDs and piperazine ring, as well between the hydroxyl and carboxyl or fluorine of NOR/CIP. Besides, the carbon on the aromatic ring also has a relatively strong electron-withdrawing ability, the Ar-H…O hydrogen bond also can be formed. On the other hand, charge transfer also plays an important role. It can be also related to the electron accepting nature of the $–SO_3H$ groups, and the electron donating character of the target FQs. The conjugation system of NOR/CIP can be connected to S-CDs by charge transfer. The introduction of NOR/CIP to S-CDs may promote the polymerization of C=C bonds. As shown in Fig. 3a, Fig. S5 and Fig. S6, compared with S-CDs blank, the UV-Vis absorption and fluorescence intensity of S-CDs + NOR/CIP are markedly enhanced but the wavelength is almost no changed. The synergy effect of the hydrogen bond and charge transfer can promote the generation of larger chromophores and fluorophores. The conjugates produce more intense emission under same excitation [29, 31, 36, 40].

Sensitivity and selectivity measurements

Under the optimized condition, the fluorescence emission spectra of S-CDs + NOR/CIP system with different concentrations of NOR and CIP added were measured. As shown in Fig. S5 and Fig. S6, the fluorescence intensity sharply increased along with

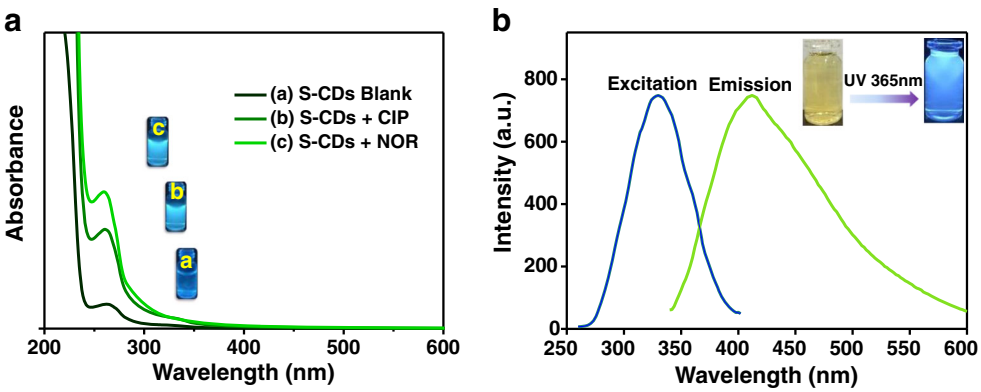

Fig. 3 a UV-Vis absorption spectra of the (a) S-CD solution black, (b) S-CDs + CIP mixture, (c) S-CDs + NOR mixture. The strong absorption peak was located at 262 nm. b Fluorescence excitation and emission spectra of S-CDs, the excitation/emission maxima at 324/412 nm. The insert is a photograph of S-CD solution under sunlight (left) and 365 nm UV light (right), respectively

the increasing concentration of NOR and CIP from 0 to 2.0 μM, but had no effect on the shape of fluorescence spectrum, which revealed the assay was very sensitive to NOR and CIP.

In order to prove the selectivity of the method, the selectivity of extractions by the MNPs was investigated. In conclusion, some potential interferences such as some metal ions, tetracycline and other organic pollutants (or hormone) can hardly be adsorbed. As far as we know, no literature reports that this magnetic nanoparticles was used to adsorb these potential interferences. It proves the practicability of adsorption method. Furthermore, to investigate the selectivity of S-CDs toward different FQs residues, including ofloxacin (OFL), difloxacin (DIF), fleroxacin (FLE), pefloxacin (PEF), enoxacin (ENO), levofloxacin (LEV), norfloxacin (NOR), and ciprofloxacin (CIP). The fluorescent properties of S-CD aqueous solution under diverse FQs residues were examined. The influence of other FQs residues on the fluorescent behavior of S-CDs is evaluated as depicted in Fig. 4.The fluorescence intensity remained nearly unchanged when the foreign substances was added. And fluorescence enhancement only occurred in the system containing NOR or CIP. The possible reasons of high selectivity is described as follows: FQs is a fluorinated 4-quinolone ring containing carboxylic acid, fluorine and a piperazine ring substitution at position 3, 7 and 8. Strong hydrogen bond occurs between the carboxyl of S-CDs and amine of the piperazine ring preferentially [41]. Also, this strong hydrogen bond plays a major role in all hydrogen bond "bridge". Besides, quinolone ring is the essential conjugation system of FQs, charge transfer occurs between the quinolone ring and S-CDs. However, as shown in Table S1, the difference between all molecular structures was proposed. For most FQs, the amine of the piperazine ring was substituted by methyl, which leads to the strong hydrogen bond can't be formed. It is negative for charge transfer and further hinders the production of sensitization. In addition, the benzene ring in the quinolone ring was replaced by a pyridine ring. The conjugation system and electron donating character of FQs were weakened, such as ENO. Thus, the system allows for the specific determination of NOR and CIP even in the presence of the potentially interfering substances mentioned above.

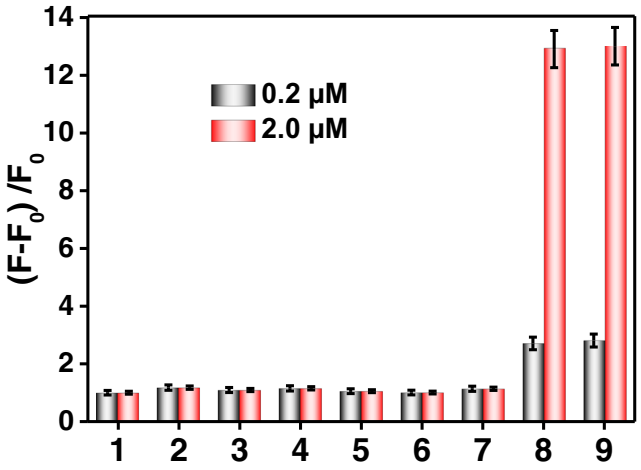

Fig. 4 The fluorescence enhancement effect of different FQs towards S-CDs with different concentrations: 0.2 μM (black column) and 2.0 μM (red column). From left: 1. S-CDs blank, 2. OFL, 3. DIF, 4. FLE, 5. PEF, 6. ENO, 7. LEV, 8. CIP, 9. NOR. The data was acquired at excitation/emission peaks of 324/412 nm

Optimization for the determination of CIP & NOR

The fluorescence enhancement efficiency of the assay system closely relied on some experimental conditions. In this work, we optimized the pH value of aqueous solutions, and incubation time of the assay system. As shown in Fig. S7, the fluorescence intensity of S-CDs (with excitation/emission maxima at 324/412 nm) was investigated under various pH solutions (2.0 to 12.0). An increase in pH from 2.0 to 6.0 results in the increased fluorescence enhancement efficiency of the established system, whereas a further increase in pH from 6.0 to 12.0 leads to a gradual decrease. Such an observation suggests that the fluorescence intensity of the S-CDs strongly depends on the pH value of the system. In the experiments, the carboxyl, hydroxyl and sulfonyl groups may be protonated in acidic solutions, which will lead to the aggregation of S-CDs, resulting in the fluorescence quenching at low pH value. On the other hand, the results may be attributed to neutralization reaction in alkaline solution [42]. This phenomenon further confirms that the carboxyl, hydroxyl and sulfonyl groups are present on the surface of S-CDs. These functional group endow the S-CDs with reasonable hydrophilic properties, stability and dispersibility in water. Consequently, we selected 6.0 as the optimal pH for our study.

We sequentially optimized the incubation time. The effect of incubation time on the fluorescence intensity of the system is shown in Fig. S8. The fluorescence intensity with excitation/emission maxima at 324/412 nm was recorded from 0 to 30 min. No significant changes in fluorescence intensity were observed after an incubation time of 10 min. To ensure the consistency of the whole experiment, it is important to record the stable fluorescence signal. Thus, 10 min is conservatively chosen as the optimum incubation time.

Norfloxacin (NOR) and ciprofloxacin (CIP) detection

Under the optimized condition, different concentrations of NOR and CIP solution were added to the S-CD solution, respectively. The fluorescence emission intensity at 412 nm was measured to study the sensitivity of the S-CDs. With the increase of NOR and CIP, the fluorescence intensity of the S-CDs at 412 nm increased gradually. As shown in Fig. 5a and b, the value of log (F/F_0) increased gradually with increasing

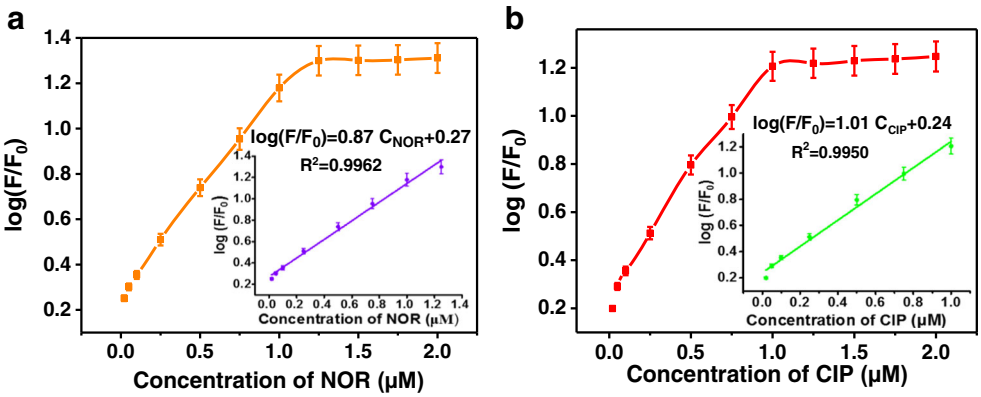

Fig. 5 The relationship between log (F/F_0) and the concentration of (a) NOR (calibration curve showing the linear dependence of log (F/F_0) values on the concentration from 0.02 to 1.25 μM. ($n = 3$)). (b) CIP (calibration curve showing the linear dependence of log (F/F_0) values on the concentration from 0.02 to 1.0 μM. (n = 3)). The data was acquired at excitation/emission peaks of 324/412 nm

NOR or CIP concentration. The linear calibration in the range from 0.02 to 1.25 μM and 0.02 to 1.0 μM, log (F/F_0) = 0.87 C_{NOR} + 0.27 and log (F/F_0) = 1.01 C_{CIP} + 0.24 were obtained, respectively, where F_0 and F were the fluorescence intensities of S-CDs at 412 nm in the absence and presence of NOR or CIP. And the limit of detection was estimated to be 4.6 nM (NOR) and 6.7 nM (CIP) based on three times signal-to-noise ratio. The results demonstrate that the method can be employed as an excellent alternative for trace analysis of NOR or CIP.

Real sample detection

In order to prove the practical applicability in real sample analysis, this system was applied to norfloxacin and ciprofloxacin residues determination in bovine raw milk samples. The corresponding results of fluorescence measurements before and after the standard addition method were listed in Table 1. The average recoveries of norfloxacin and ciprofloxacin residues in bovine raw milk samples were 96.2%~105.2% and 92.3%~102.5%, respectively. Relative standard deviations (RSDs) of the two compounds of samples were both found lower than 3.7%.

Moreover, the same samples were analyzed simultaneously by fluorescence enhancement detection without MSPE for comparison. As listed in Table 1, in terms of average recoveries and relative standard deviations (RSDs), it can be concluded that the analytical performance of the method was obviously better than fluorescence enhancement detection without MSPE. It proves MSPE is a necessary part in this method. Compared with the published methods for the determination of FQs, our method shows higher sensitivity, lower LODs (Table 2).Therefore, it is expected that the results summarized in Table 1 further demonstrated the practical value of this method for norfloxacin and ciprofloxacin residues in real samples.

Conclusion

In conclusion, a novel assay for detection of norfloxacin (NOR) and ciprofloxacin (CIP) was constructed by the combination of fluorescence enhancement technology and magnetic solid-phase extraction (MSPE). Based on the strong hydrogen bond interaction and charge transfer between S-CDs and NOR/CIP, the fluorescence probe exhibits excellent

Table 1 Determination of NOR and CIP residues in bovine raw milk samples using the fluorescence enhancement method ($n = 3$)

samples	Spiked milk						
	Spiked level (μM)	Found[a] (μM)	Found[b] (μM)	Recoveries[a] (%)	Recoveries[b] (%)	RSD[a] (%)	RSD[b] (%)
NOR	0	nd[c]	nd[c]	–	–	–	–
	0.05	0.048	0.042	96.2	84.3	3.7	7.5
	0.2	0.21	0.17	105.2	88.4	1.8	6.9
	0.8	0.79	0.73	98.8	90.9	2.8	5.1
CIP	0	nd[c]	nd[c]	–	–	–	–
	0.05	0.048	0.042	96.3	85.6	3.2	7.2
	0.2	0.18	0.17	92.3	87.2	2.7	6.2
	0.8	0.82	0.74	102.5	92.4	1.0	5.4

[a] Determination by the proposed method (μM)

[b] Fluorescence detection without MSPE (μM)

[c] nd defined as "not detection"

Table 2 The comparison of different analytical methods for the determination of FQs

Method	analyte	Linear range	Detection Limit	Real sample	Ref.
Colorimetry	CIP	4–500 nM	1.2 nM	water, serum, milk	[1]
HPLC/ post-column derivatization	CIP	7.2–900 ng·mL^{-1}	2.5 ng·mL^{-1}	milk	[7]
SERS	Levo	1–15 μM	0.8μM	water	[8]
HPLC-FLD	NOR	200–2000 μg·L^{-1}	150 μg·L^{-1}	surface water	[9]
	CIP	200–2000 μg/L	100 μg/L	surface water	[9]
LC-MS/MS	Enrofloxacin	0.5–50 ng·mL^{-1}	0.22 ng·mL^{-1}	Milk-based Powders	[10]
Spectrofluorimetric	NOR	0.038–10.0 μM	0.021 μM	fish, chicken	[14]
Fluorescence	NOR	0.02–1.25 μM	4.6 nM	bovine raw milk	This work
	CIP	0.02–1.0 μM	6.7 nM	bovine raw milk	This work

selectivity and sensitivity towards analytes. Moreover, the analytical method was successfully used to detect NOR or CIP in real milk samples with a detection limit of 4.6 nM (NOR) and 6.7 nM (CIP). To the best of our knowledge, this is the first time that there has been report on the use of fluorescent S-CDs for detection of NOR or CIP residues coupled with magnetic solid-phase extraction. We believe that the property of distinguishing NOR from CIP in real samples by CDs probe will be promising in wider scope.

Acknowledgements This study was supported by the Analysis and Testing Foundation (No. 2017 M 20162118079) of Kunming University of Science and Technology, Yunnan Province, China.

Compliance with ethical standards The author(s) declare that they have no competing interests.

References

1. Lavaee P, Danesh NM, Ramezani M, Abnous K, Taghdisi SM (2017) Colorimetric aptamer based assay for the determination of fluoroquinolones by triggering the reduction-catalyzing activity of gold nanoparticles. Microchim Acta 184(7):2039–2045
2. Pico Y, Andreu V (2007) Fluoroquinolones in soil-risks and challenges. Anal Bioanal Chem 387(4):1287–1299
3. Liu X, Steele JC, Meng X-Z (2017) Usage, residue, and human health risk of antibiotics in Chinese aquaculture: a review. Environ Pollut 223:161–169
4. Li ZM, Li ZH, Zhao DY, Wen F, Jiang JD, Xu DK (2017) Smartphone-based visualized microarray detection for multiplexed harmful substances in milk. Biosens Bioelectron 87(15):874–880
5. Wang C, Li XM, Peng T, Wang ZH, Wen K, Jiang HY (2017) Latex bead and colloidal gold applied in a multiplex immunochromatographic assay for high-throughput detection of three classes of antibiotic residues in milk. Food Control 77:1–7
6. Li QZ, Gao JX, Zhang QL, Liang LZ, Tao H (2017) Distribution and risk assessment of antibiotics in a typical river in North China plain. Bull Environ Contam Toxicol 98(4):478–483
7. Yanez-Jacome GS, Aguilar-Caballos MP, Gomez-Hens A (2015) Luminescent determination of quinolones in milk samples by liquid chromatography/post-column derivatization with terbium oxide nanoparticles. J Chromatogr A 1405(31):126–132
8. Hidi IJ, Jahn M, Weber K, Cialla-May D, Popp J (2015) Droplet based microfluidics: spectroscopic characterization of levofloxacin and its SERS detection. Phys Chem Chem Phys 17(33):21236–21242
9. Jin T, Wu H, Gao NN, Chen XD, Lai HJ, Zheng JF, Du LM (2016) Extraction of quinolones from milk samples using bentonite/magnetite nanoparticles before determination by high-performance liquid chromatography with fluorimetric detection. J Sep Sci 39(3):545–551
10. Wittenberg JB, Simon KA, Wong JW (2017) Targeted multiresidue analysis of veterinary drugs in milk-based powders using liquid chromatography-tandem mass spectrometry (LC-MS/MS). J Agric Food Chem 65(34):7288–7293
11. Huang J-Y, Bao T, Hu T-X, Wen W, Zhang X-H, Wang S-F (2017) Voltammetric determination of levofloxacin using a glassy carbon electrode modified with poly(o-aminophenol) and graphene quantum dots. Microchim Acta 184(1):127–135
12. Amjadi M, Manzoori JL, Hallaj T, Shahbazsaghir T (2017) Application of the chemiluminescence system composed of silicon-doped carbon dots, iron(II) and $K_2S_2O_8$ to the determination of norfloxacin. Microchim Acta 184(6):1587–1593
13. Xia QH, Yang YL, Liu MS (2012) Aluminium sensitized spectrofluorimetric determination of fluoroquinolones in milk samples coupled with salting-out assisted liquid-liquid ultrasonic extraction. Spectrochim Acta A 96:358–364
14. Duan RL, Jiang JZ, Liu SP, Yang JD, Qiao M, Shi Y, Hu XL (2017) Determination of norfloxacin in food by an enhanced spectrofluorimetric method. J Sci Food Agr 97(8):2569–2574
15. Mao BB, Qu F, Zhu SY, You JM (2016) Fluorescence turn-on strategy based on silver nanoclusters-Cu^{2+} system for trace detection of quinolones. Sens Actuator B Chem 234(29):338–344
16. Xu SM, Liu Y, Yang H, Zhao K, Li JG, Deng AP (2017) Fluorescent nitrogen and sulfur co-doped carbon dots from casein and their applications for sensitive detection of Hg^{2+} and biothiols and cellular imaging. Anal Chim Acta 964(29):150–160
17. Wu D, Li GL, Chen XF, Qiu NN, Shi XX, Chen GA, Sun ZW, You JM, Wu YN (2017) Fluorometric determination and imaging of glutathione based on a thiol-triggered inner filter effect on the fluorescence of carbon dots. Microchim Acta 184(7):1923–1931

18. Thambiraj S, Shankaran DR (2016) Green synthesis of highly fluorescent carbon quantum dots from sugarcane bagasse pulp. Appl Surf Sci 390(30):435–443
19. Shi BF, Su YB, Zhang LL, Huang MJ, Liu RJ, Zhao SL (2016) Nitrogen and phosphorus co-doped carbon Nanodots as a novel fluorescent probe for highly sensitive detection of Fe^{3+} in human serum and living cells. ACS Appl Mater Interfaces 8(17):10717–10725
20. Sun XC, Bruckner C, Lei Y (2015) One-pot and ultrafast synthesis of nitrogen and phosphorus co-doped carbon dots possessing bright dual wavelength fluorescence emission. Nano 7(41):17278–17282
21. Xiao Q, Liang Y, Zhu FW, Lu SY, Huang S (2017) Microwave-assisted one-pot synthesis of highly luminescent N-doped carbon dots for cellular imaging and multi-ion probing. Microchim Acta 184(7):2429–2438
22. Zhu SJ, Meng QN, Wang L, Zhang JH, Song YB, Jin H, Zhang K, Sun HC, Wang HY, Yang B (2013) Highly Photoluminescent carbon dots for multicolor patterning, sensors, and bioimaging. Angew Chem Int Edit 52(14):3953–3957
23. Liu YL, Zhou QX, Li J, Lei M, Yan XY (2016) Selective and sensitive chemosensor for lead ions using fluorescent carbon dots prepared from chocolate by one-step hydrothermal method. Sens Actuator B Chem 237:597–604
24. Rao HB, Ge HW, Wang XX, Zhang ZY, Liu X, Yang Y, Liu YQ, Liu W, Zou P, Wang YY (2017) Colorimetric and fluorometric detection of protamine by using a dual-mode probe consisting of carbon quantum dots and gold nanoparticles. Microchim Acta 184(8):3017–3025
25. Devi JSA, Anulekshmi AH, Salini S, Aparna RS, George S (2017) Boronic acid functionalized nitrogen doped carbon dots for fluorescent turn-on detection of dopamine. Microchim Acta 184(10):4081–4090
26. Zhang L, Zhang Z-Y, Liang R-P, Li Y-H, Qiu J-D (2014) Boron-doped graphene quantum dots for selective glucose sensing based on the "abnormal" aggregation-induced photoluminescence enhancement. Anal Chem 86(9):4423–4430
27. Qian ZS, Shan XY, Chai LJ, Ma JJ, Chen JR, Feng H (2014) Si-doped carbon quantum dots: a facile and general preparation strategy, bioimaging application, and multifunctional sensor. ACS Appl Mater Interfaces 6(9):6797–6805
28. Miao H, Wang L, Zhuo Y, Zhou ZN, Yang XM (2016) Label-free fluorimetric detection of CEA using carbon dots derived from tomato juice. Biosens Bioelectron 86(15):83–89
29. Sun XC, Lei Y (2017) Fluorescent carbon dots and their sensing applications. TrAC Trends Anal Chem 89:163–180
30. Wu JS, Liu WM, Ge JC, Zhang HY, Wang PF (2011) New sensing mechanisms for design of fluorescent chemosensors emerging in recent years. Chem Soc Rev 40(7):3483–3495
31. Algar WR, Tavares AJ, Krull UJ (2010) Beyond labels: a review of the application of quantum dots as integrated components of assays, bioprobes, and biosensors utilizing optical transduction. Anal Chim Acta 673(1):1–25
32. Zu FL, Yan FY, Bai ZJ, Xu JX, Wang YY, Huang YC, Zhou XG (2017) The quenching of the fluorescence of carbon dots: a review on mechanisms and applications. Microchim Acta 184(7):1899–1914
33. Xu S, Jiang C, Lin YX, Jia L (2012) Magnetic nanoparticles modified with polydimethylsiloxane and multi-walled carbon nanotubes for solid-phase extraction of fluoroquinolones. Microchim Acta 179(3–4):257–264
34. Zhang HJ, Qiao X, Cai TP, Chen J, Li Z, Qiu HD (2017) Preparation and characterization of carbon dot-decorated silica stationary phase in deep eutectic solvents for hydrophilic interaction chromatography. Anal Bioanal Chem 409(9):2401–2410
35. Cai TP, Zhang HJ, Rahman AFMM, Shi Y-P, Qiu HD (2017) Silica grafted with silanized carbon dots as a nano-on-micro packing material with enhanced hydrophilic selectivity. Microchim Acta 184(8):2629–2636
36. Qin H, Qiu XY, Zhao J, Liu MS, Yang YL (2013) Supramolecular solvent-based vortex-mixed microextraction: determination of glucocorticoids in water samples. J Chromatogr A 1311(11):11–20
37. Li JJ, Jiao YZ, Feng LD, Zhong Y, Zuo GC, Xie AM, Dong W (2017) Highly N,P-doped carbon dots: rational design, photoluminescence and cellular imaging. Microchim Acta 184(8):2933–2940
38. Liu YH, Duan WX, Song W, Liu JJ, Ren CL, Wu J, Liu D, Chen HL (2017) Red emission B, N, S-co-doped carbon dots for colorimetric and fluorescent dual mode detection of Fe^{3+} ions in complex biological fluids and living cells. ACS Appl Mater Interfaces 9(14):12663–12672
39. Travlou NA, Secor J, Bandosz TJ (2017) Highly luminescent S-doped carbon dots for the selective detection of ammonia. Carbon 114:544–556
40. Serna-Galvis EA, Jojoa-Sierra SD, Berrio-Perlaza KE, Ferraro F, Torres-Palma RA (2017) Structure-reactivity relationship in the degradation of three representative fluoroquinolone antibiotics in water by electrogenerated active chlorine. Chem Eng J 315(1):552–561
41. Prutthiwanasan B, Phechkrajang C, Suntornsuk L (2016) Fluorescent labelling of ciprofloxacin and norfloxacin and its application for residues analysis in surface water. Talanta 159(1):74–79
42. Wang RX, Wang XF, Sun YM (2017) One-step synthesis of self-doped carbon dots with highly photoluminescence as multifunctional biosensors for detection of iron ions and pH. Sens Actuator B Chem 241(31):73–79